Surface aerosol radiative forcing at Gosan during the ACE-Asia campaign

Brett C. Bush and Francisco P. J. Valero

Atmospheric Research Laboratory, Scripps Institution of Oceanography, University of California, San Diego, La Jolla, California, USA

Received 27 November 2002; revised 21 February 2003; accepted 27 March 2003; published 26 August 2003.

[1] Surface radiation measurements were made at Gosan, Jeju, Republic of Korea, during the ACE-Asia field campaign aimed at assessing the impact of aerosols, specifically the "Asian yellow dust," throughout the region. Downwelling total, direct, and diffuse radiative fluxes were measured in the total solar spectrum as well as near-infrared and visible portions of the spectrum. Aerosol optical depth measurements at 500 nm were also made using a scanning shadow band radiometer. Surface radiative forcing values were determined during clear-sky conditions made from 25 March to 4 May 2001. The diurnal forcing efficiency, determined by taking the slope of the best fit line through the flux versus optical depth plot, was found to be -73.0 ± 9.6, -35.8 ± 5.5, and -42.2 ± 4.8 W m^{-2}/τ_{500} for the total solar, near-infrared, and visible spectral regions. We also introduce a new radiative forcing parameter, the fractional forcing efficiency, defined to express the radiative forcing relative to the total energy incident at the top of the atmosphere. The fractional diurnal forcing efficiency at Gosan during ACE-Asia was -18.0 ± 2.3, -16.2 ± 2.4, and $-26.7 \pm 3.3\%/\tau_{500}$ for the same band passes, indicating that a larger percentage of the flux at visible wavelengths is radiatively forced compared to the total and near-infrared portions of the solar spectrum. *INDEX TERMS:* 0305 Atmospheric Composition and Structure: Aerosols and particles (0345, 4801); 0360 Atmospheric Composition and Structure: Transmission and scattering of radiation; 0394 Atmospheric Composition and Structure: Instruments and techniques; *KEYWORDS:* radiative fluxes, radiative forcing, aerosols

Citation: Bush, B. C., and F. P. J. Valero, Surface aerosol radiative forcing at Gosan during the ACE-Asia campaign, *J. Geophys. Res.*, *108*(D23), 8660, doi:10.1029/2002JD003233, 2003.

1. Introduction

[2] The Asian-Pacific Regional Aerosol Characterization Experiment (ACE-Asia) was a multi-platform project based throughout Asia that was designed to increase the understanding of how aerosol particles affect the Earth's climate system. The combination of satellite, airborne, and surface (land and ship) measurements was designed to monitor the variability in magnitude and composition as well as the geographic distribution of natural and anthropogenic aerosols over the entire atmospheric column. The measurements from the various platforms allowed air masses to be tracked from the onset of large dust events at the surface in the source region to in situ measurements assessing the aging processes of the particles. ACE-Asia is the continuation of a series of Aerosol Characterization Experiments planned by the International Global Atmospheric Chemistry Program (IGAC) [*Bates et al.*, 1998; *Bates*, 1999; *Raes et al.*, 2000; *Rodhe*, 2000; *Huebert*, 2001].

[3] One of the major ground stations during ACE-Asia was at Gosan (33.29°N, 126.16°E) on the island of Jeju, Republic of Korea. The site was located at the western edge of the island at the top of a cliff about 50 meters directly above the East China Sea. The prevailing surface winds were typically from the seaward direction thus isolating the site from local pollution sources. A variety of instrumentation existed at Gosan including but not limited to measurements of aerosol and gas chemistry and composition, particle number concentration and size distribution, as well as radiation fluxes and optical depths in a range of band passes and specific wavelengths. This combination of instruments at Gosan made it a very comprehensive site for studying the effects of aerosols in the region.

[4] One major goal in making the radiation measurements at Gosan was to quantify the relationship between aerosols and the surface fluxes in this region. The changes in the radiative fluxes, or radiative forcings, due to the varying aerosol quantity and composition are critical factors that drive climatic processes on both planetary and local scales [*Graham*, 1995]. At the surface, the radiative fluxes are dependent on the entire atmospheric column that interacts with the solar radiation. Understanding the radiative forcings and forcing efficiencies is essential in better understanding the major sources of uncertainty in modeling climate change in global circulation models [*Hansen et al.*, 1998].

2. Radiometric Measurements

[5] All of the radiometric measurements described in this study are taken from RAMS (Radiometric Measurement

0148-0227/03/2002JD003233$09.00

Table 1. RAMS Instrumentation Summary

Instrument	FOV	Band Pass	Accuracy
TSBR	hemispherical	0.3–3.8 μm	1%
FSBR	hemispherical	0.68–3.3 μm	1%
TDDR	hemispherical	0.40–0.70 μm	3%
DTSBR	±2.8°	0.3–3.8 μm	0.5%

System) that has been used extensively in a variety of field campaigns [*Valero et al.*, 1982, 1997; *Bush et al.*, 1999; *Valero and Bush*, 1999; *Bush and Valero*, 2002; *Valero et al.*, 2003]. In this project, the RAMS surface platform consisted of four radiometers: three with hemispherical fields-of-view that measured the downwelling flux at the surface, and one narrow field-of-view instrument that was mounted on a solar tracker to measure the direct solar beam radiance from sunrise to sunset. Two of the three hemispherical field-of-view instruments measured broadband portions of the solar spectrum. The TSBR, total solar broadband radiometer, covered the spectral region from approximately 0.3–3.8 μm, and the FSBR, fractional solar broadband radiometer, covered the 0.68–3.3 μm spectral region. The third hemispherical field-of-view instrument measured the visible portion of the solar spectrum from 400 to 700 nm using six 50 nm band-pass channels, with an additional 10 nm narrowband channel centered at 500 nm for use in calculating optical depths. This instrument, the TDDR or total direct diffuse radiometer, also had a shadow band that oscillated with a period of approximately 1 min so that under clear sky conditions the direct component of the solar flux in each of the spectral channels could be determined. The final instrument that was mounted on the solar tracker, the DTSBR or direct TSBR, was identical to the TSBR flux instrument except for the field-of-view restriction of ±2.8° that was centered on the solar disk throughout each day. A summary of the RAMS instrumentation is given in Table 1 along with their absolute accuracy. RAMS acquired data at a rate of approximately 2 Hz. An example of the RAMS measurements at Gosan on day 105 (15 April 2001) during ACE-Asia is given in Figure 1 for a predominantly clear sky day.

[6] The combination of the RAMS instrumentation described above provides a means of calculating a variety of radiometric quantities other than the radiance and irradiances directly measured. The diffuse component of the total solar flux is determined by subtracting the direct solar component from the global flux, both quantities being directly measured. Analysis of the TDDR measurement gives the global, direct, diffuse, and forward-scattered components of the visible flux on a time scale comparable to the period of the scanning shadow band. (See *Bush and Valero* [2002] for a complete description.) Furthermore, there is a redundancy in some of the measurements because the combination of the TDDR visible measurement (0.40–0.70 μm) and the FSBR near infra-red measurement (0.68–3.3 μm) is approximately equal to that of the TSBR measurement (0.3–3.8 μm) provided that flux in the "missing" spectral regions is considered.

[7] Spectral aerosol optical depths are determined directly from the RAMS measurements. The measured direct solar flux from the TDDR 500 nm narrowband channel and the modeled top of atmosphere (TOA) value are used to determine the line-of-sight (LOS) extinction. The Rayleigh component and that from minor atmospheric constituents (e.g., ozone) are removed when determining the aerosol component of this total optical depth. The LOS optical depth is then converted to the vertical optical depth using the known location of the Sun. Hereafter, all references to the aerosol optical depth represent this quantity, τ_{500}, at a wavelength of 500 nm.

[8] The TDDR 500 nm optical depths are screened in order to represent primarily clear-sky conditions. In the screening process, a linear fit to the DTSBR measurement is made for a time period consisting of 20 min about each measurement time. The difference between the DTSBR measurement and this fit is then determined. This difference represents the variation of the direct solar flux after removing the recent local zenith angle variations of the Sun. When both the instantaneous value of this difference is less than 1.0% (relative to the average DTSBR measurement for the 20 min period) and the standard deviation of the entire set of differences within the 20 min sample period is also less than 1.0%, the measurement time is flagged as being "clear". In the clear-sky radiative forcing calculations described below, the additional requirement that the diffuse flux, derived from the TDDR measurement in the 400 to 700 nm spectral region, be invariant for the same 20 min time period about the measurement is imposed.

[9] A histogram of τ_{500} over all the clear sky conditions measured by RAMS at the Gosan site during ACE-Asia is given in Figure 2. The majority of the aerosol optical depths during this period were in the 0.3–0.5 range. There were also some relatively clean cases where τ_{500} was about 0.1–0.15 (day 106, 16 April 2001) and some high aerosol events in which τ_{500} was over 0.6 (day 103, 13 April 2001). Coincident with the RAMS aerosol optical depth measurements made at Gosan during ACE-Asia, there were with three other independent measurements made by the Aerosol Robotic Network (AERONET) [*Holben et al.*, 1998], the Meteorological Research Institute (METRI) (J.Y. Kim, private communication, 2001), and the National Oceanic and Atmospheric Administration, Climate Monitoring and Diagnostics Laboratory (NOAA/CMDL) (S. W. Kim, pri-

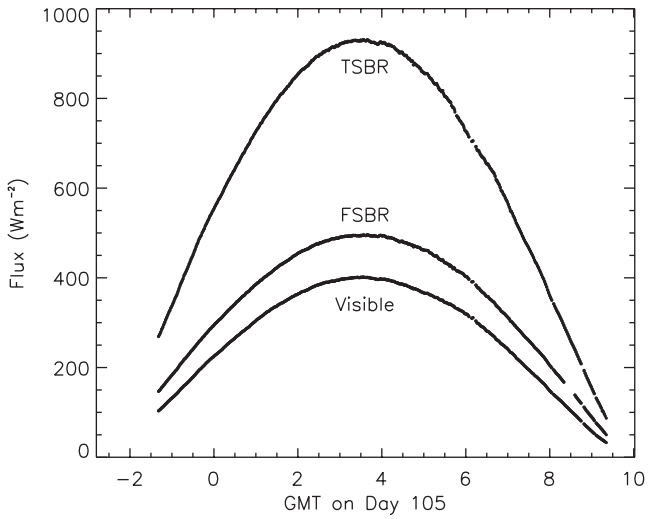

Figure 1. RAMS measurements at Gosan on day 105 (15 April 2001). The TSBR, FSBR, and visible flux measurements are shown.

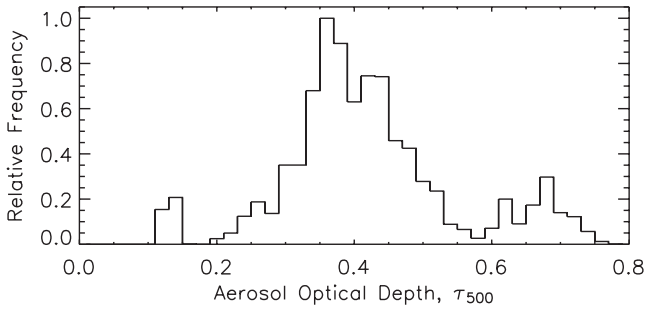

Figure 2. Histogram of τ_{500} at Gosan for the entire ACE-Asia field campaign.

vate communication, 2002). Given the 3% accuracy (see Table 1) of the TDDR flux measurements used in determining the 500 nm aerosol optical depth, the associated uncertainty in τ_{500} is about 0.03 for the RAMS measurements. Table 2 gives a statistical comparison of the AERONET, METRI, and NOAA/CMDL aerosol optical depths relative to the RAMS values. For each of the independent measurements, both absolute aerosol optical depths differences as well as the RMS deviations are consistent (within measurement uncertainties) with the RAMS optical depths. Later, it is shown that the surface forcing parameters are independent of the particular aerosol optical depth measurement applied in this study.

3. Aerosol Radiative Forcing at the Surface

[10] Surface aerosol radiative forcing is defined as the difference between the net flux at the surface and the same quantity when there is no-aerosol present in the atmosphere. In other words, it is the perturbation in the surface net flux due to the presence of an aerosol in all of the atmospheric layers above. Radiative forcing, ΔF, is expressed as:

$$\Delta F = F_{net} - F^0_{net}, \tag{1}$$

where, the net flux is the difference between the downwelling flux, $F_{\downarrow}$, and upwelling flux, $F_{\uparrow}$:

$$F_{net} = F\downarrow - F\uparrow . \tag{2}$$

When the upwelling surface flux is not directly measured, we can estimate it in terms of the downwelling flux and the surface albedo, α, via:

$$F\uparrow = \alpha \times F\downarrow . \tag{3}$$

Thus combining (2) and (3), the net flux at the surface is expressed as:

$$F_{net} = (1 - \alpha) \times F\downarrow . \tag{4}$$

Since there are no direct measurements of the pristine (no-aerosol) downwelling surface fluxes during the ACE-Asia field campaign at the Gosan site, this quantity is calculated using the MODTRAN 4.0 atmospheric model [*Anderson et al.*, 1999]. Previous studies have shown that the aerosol composition, optical parameterization, and distribution of aerosols can be a significant source of error in clear sky radiative transfer model calculations [*Valero and Bush*, 1999]. The uncertainties in the modeled fluxes are reduced in this calculation due to the restriction that there are no-aerosols present in the atmosphere; this is particularly true in the visible region of the spectrum where the effects of water vapor are also small. The model calculations completed in this study use the atmospheric soundings of temperature, pressure, and water vapor provided by the METRI and the Korean Meteorological Administration (KMA) (J.Y. Kim, private communication, 2001).

[11] The results of the no-aerosol model run on 13 and 16 April 2001 are presented in Figures 3a and 3b, respectively, as the dashed lines. The observations indicate that the largest aerosol optical depths occurred on 13 April and that the lowest values occurred on 16 April. In both cases, the no-aerosol calculations are always greater than the measured fluxes. For reference, the TOA values (dotted lines) are also shown for each spectral region. The radiative forcing at the surface is calculated from the measurements and model results using equations (1) and (4). A slight solar zenith angle dependence exists in the radiative forcing term, but it is not as pronounced as that in the flux values.

[12] For all of the forcing calculations, the surface albedoes (over water) are estimated as 3.0 ± 0.2%, 2.5 ± 0.2%, and 3.8 ± 0.3% for the TSBR, FSBR, and visible band passes, respectively. These albedo values are measured using identical instrumentation to RAMS from the airborne platform aboard the NCAR C-130 that operated during ACE-Asia. These albedo measurements correspond to averages over 12 days during the ACE-Asia campaign when the C-130 was flying under clear skies at low altitude (less than 200 m) over water. The relatively small variability in the albedo measurements over the entire ACE-Asia period indicates that conditions such as wind speed, etc., do not significantly affect this parameter and, in turn, are a minor contribution to the uncertainties in the forcing calculations.

[13] In this work, as well as in previous studies [*Jayaraman et al.*, 1998; *Meywerk and Ramanathan*, 1999; *Bush and Valero*, 2002], although defined explicitly above, radiative forcing has been referred to in a variety of modified expressions. As expressed in equation (1), it represents the instantaneous forcing for the given measurement location and time. Although important, radiative forcing in this form is not the most useful in assessing the climatic impact of an aerosol in a region and over a prolonged period of time. Below, additional radiative forcing quantities, derived from equation (1), are defined and quantified using the radiometric measurements during ACE-Asia.

3.1. Diurnally Averaged Forcing

[14] The diurnally averaged forcing is simply the integrated radiative forcing at the surface averaged over a 24-hour period:

$$\Delta DF = \int \Delta F \, dt/24 \text{ hr}. \tag{5}$$

Table 2. Statistical Comparison of Measured Aerosol Optical Depths Relative to the RAMS Values

Platform	Average Difference	RMS Deviation
CMDL	0.019	0.016
METRI	0.017	0.026
AERONET	0.006	0.019

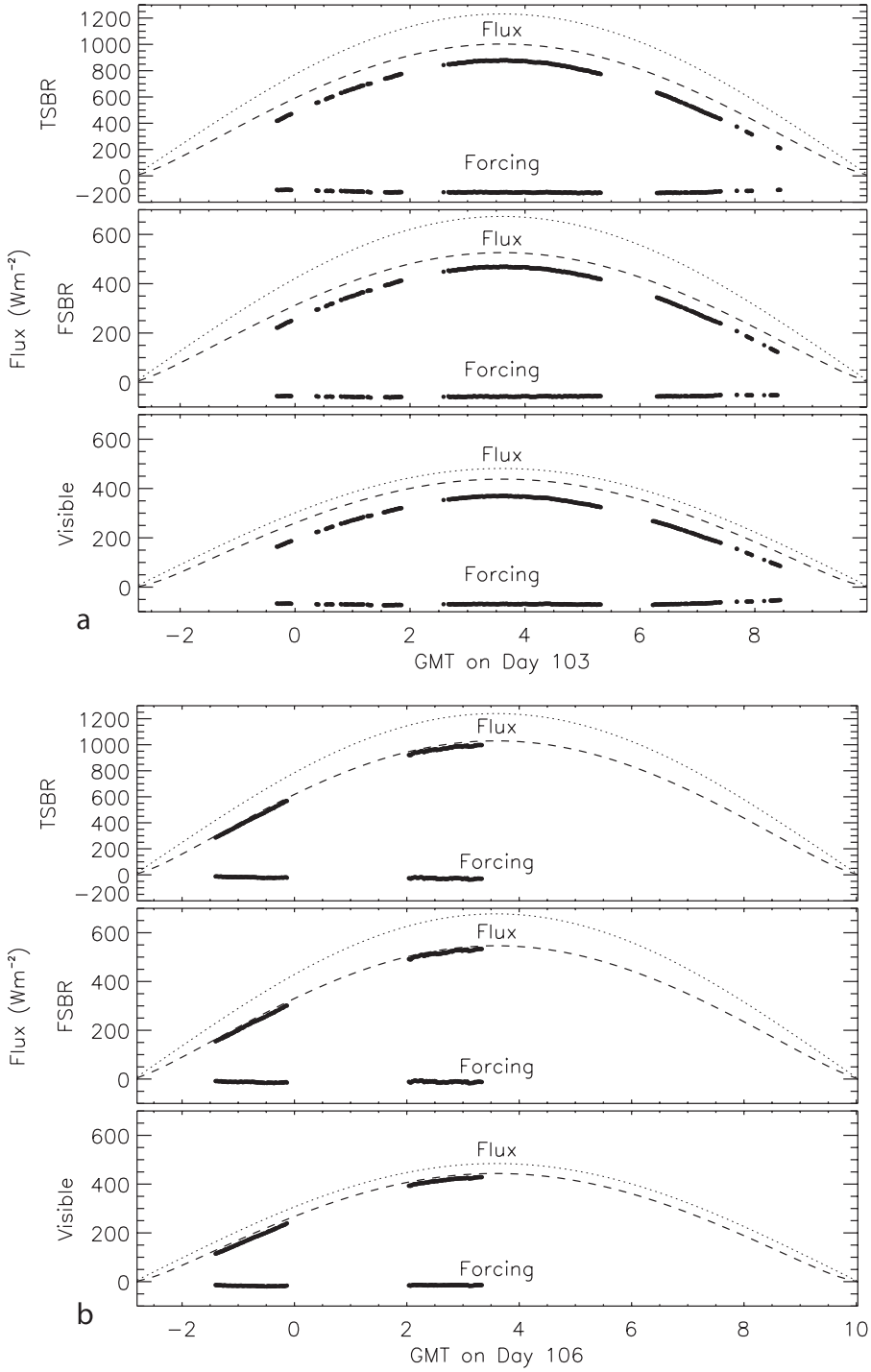

Figure 3. RAMS measurements at Gosan on (a) day 103 (13 April 2001) and (b) day 106 (16 April 2001) with the addition of the no-aerosol model runs (dashed lines). For reference, the TOA fluxes are shown as dotted lines for each spectral region. The calculated surface forcing values are also shown for each spectral region.

[15] The cases examined in this work are restricted to clear-sky conditions, so the forcing term, ΔF, must first be cloud-screened before completing the integration. After this screening is completed, the data are interpolated or extrapolated to fill in the "missing" clear-sky periods during the day. In cases where the fraction of total clear-sky conditions during the day is small, the diurnally averaged radiative forcing cannot be calculated with any reasonable certainty. In this study, we do not define a specific threshold for the percentage of clear sky throughout the day necessary for calculating a diurnal averaged forcing value, but rather assess the applicability of the data with respect to the length and time of occurrence of the non-clear segments. In most cases, the conditions are considered clear for at least 50% of the period from sunrise to sunset. For the measurements made on 13 April 2001 and depicted in Figure 3a, the diurnal

Table 3. Average Aerosol Optical Depths and Diurnal Forcing Values for Clear or Mostly Clear Days at Gosan During ACE-Asia[a]

Day	τ_{AVE}	ΔDF TSBR	ΔDF FSBR	ΔDF Visible
85 (PM)	0.353 ± 0.021	−26.0 ± 2.3	−11.3 ± 1.0	−16.0 ± 1.4
91 (AM)	0.447 ± 0.011	−30.3 ± 3.0	−15.3 ± 1.5	−18.2 ± 1.8
94 (AM)	0.309 ± 0.053	−18.3 ± 1.6	−10.6 ± 0.9	−12.0 ± 1.1
102 (PM)	0.301 ± 0.016	−31.7 ± 3.2	−13.7 ± 1.3	−17.8 ± 1.8
103 (AM,PM)	0.708 ± 0.038	−52.1 ± 2.4	−25.1 ± 1.1	−29.1 ± 1.3
105 (AM,PM)	0.357 ± 0.029	−34.0 ± 1.1	−16.9 ± 0.6	−17.2 ± 0.6
106 (AM)	0.142 ± 0.008	−10.6 ± 0.7	−5.7 ± 0.4	−7.3 ± 0.5
107 (AM,PM)	0.580 ± 0.067	−42.2 ± 1.9	−21.4 ± 1.0	−20.8 ± 0.9
108 (AM,PM)	0.415 ± 0.026	−25.6 ± 0.9	−10.4 ± 0.4	−15.7 ± 0.6
112 (AM,PM)	0.412 ± 0.071	−28.0 ± 1.1	−14.3 ± 0.6	−15.9 ± 0.7
116 (AM,PM)	0.474 ± 0.037	−36.5 ± 1.5	−18.3 ± 0.8	−19.6 ± 0.8

[a]All of the diurnal forcing values are in W m^{-2}.

average forcing is calculated to be $\Delta DF = -52.1$ W m^{-2} for the TSBR band pass.

[16] It is also instructive to calculate the average optical depth, τ_{AVE}, during the day in order to understand the relationship between the magnitudes of the diurnal forcing and average optical depth. The average 500 nm aerosol optical depth on 13 April 2001 was measured to be 0.708 ± 0.038. Even though the aerosol composition and magnitude will vary during the day, the ratio between ΔDF and τ_{AVE} will indicate the effectiveness of the aerosol in perturbing the atmosphere of the entire day - the larger the ratio, the greater the forcing per unit optical depth. This effectiveness, or forcing efficiency, is discussed in further detail below.

[17] A summary of the diurnal forcing values for 11 predominantly clear days is given in Table 3. The uncertainties in the forcing values are determined via estimates in the no-aerosol model calculations as well as albedo and radiative flux measurements. In cases when only the morning was clear, the integral in equation (5) is only completed up to the point that the Sun reaches its highest point in the sky. Similarly, when only the afternoon is clear, the integral starts at solar noon and goes for 12 hours. In both cases, the calculated value is restricted to clear sky conditions and scaled to represent a complete day. By not restricting the conditions to being mostly clear from sunrise to sunset, we are able to estimate the diurnal forcing for 11 days as opposed to only 6 without this characterization.

3.2. Fractional Forcing

[18] We introduce a new term in this work called the fractional forcing, ΔFF. This is simply the forcing, ΔF, divided by the TOA flux and represents the percentage of incident solar radiation that is being forced by the atmosphere. Both the instantaneous forcing and the diurnal

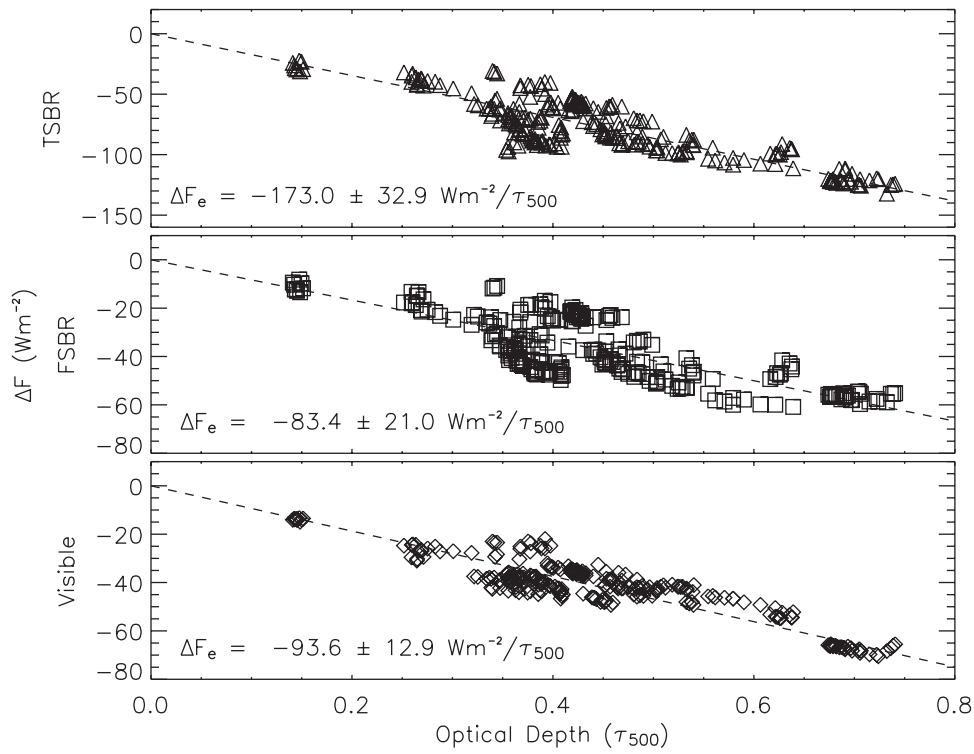

Figure 4. The radiative forcing is plotted versus the aerosol optical depth for all clear-sky data during ACE-Asia at Gosan. Each data point represents a 10-min average. The TSBR, FSBR, and visible band passes are triangles, squares, and diamonds, respectively. The dashed line represents the best fit line through the data points.

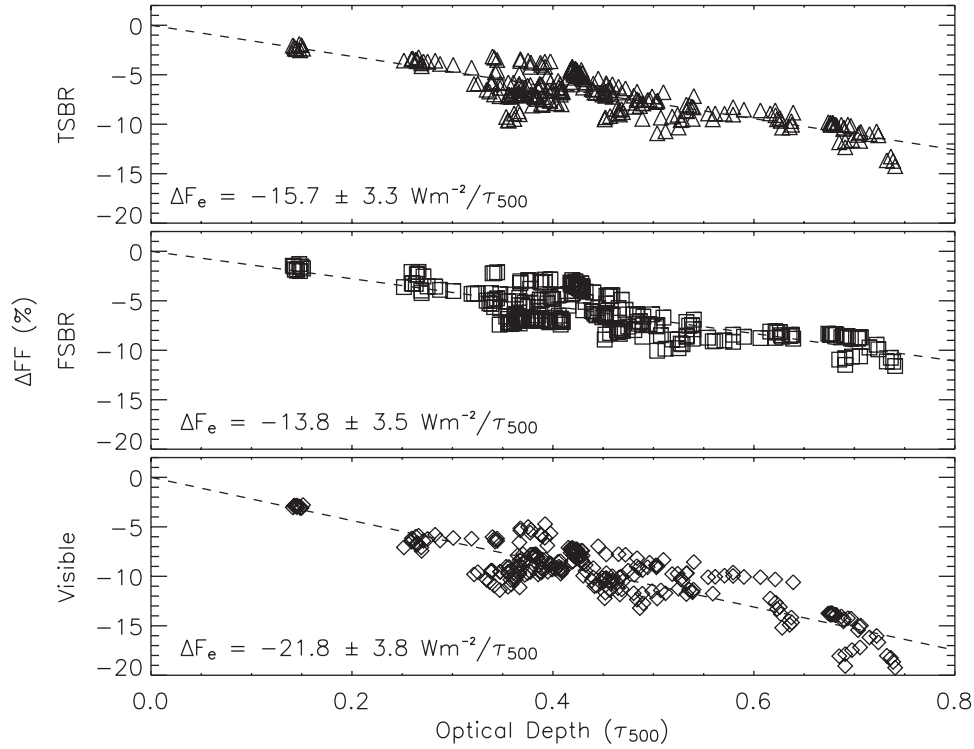

Figure 5. Same as Figure 4 but for the fractional forcing.

forcing can be expressed in fractional terms. In analogy to ΔFF, the fractional diurnal forcing, ΔFDF, is just the diurnal forcing given in equation (5) divided by the TOA solar flux that is also averaged over the same 24-hour period. On 13 April 2001 at Gosan, the average TOA flux was 415.0 W m^{-2} for the TSBR band pass indicating a ΔFDF value of -12.6% on this day. Fractional forcing and diurnal fractional forcing are more general terms that can be used to more directly compare different geographic regions or the same region at different times of the year.

3.3. Forcing Efficiency

[19] The absolute magnitude of the surface radiative forcing is highly dependent on not only the amount of energy entering the atmosphere, but also the quantity and type of aerosols perturbing the environment. As the aerosol optical depth increases, so does the radiative forcing. The rate at which the atmosphere is "forced" per unit optical depth is known as the forcing efficiency. This quantity can be calculated in absolute terms using the forcing parameters as defined in equations (1) and (5), or alternatively by their fractional forcing counterparts.

[20] Figure 4 shows ΔF plotted versus τ_{500} for the entire ensemble of data measured during ACE-Asia at Gosan. Each symbol represents a 10-min average of data and has been screened to remove clouds as described earlier. The slope of the dashed lines represent the forcing efficiency, ΔF_e, and is calculated by averaging the individual forcing efficiencies for each data point. The uncertainty of ΔF_e is the statistical standard deviation corresponding to these points. For the TSBR, FSBR, and visible band passes, the forcing efficiency is -173.0 ± 32.9, -83.4 ± 21.0, and -93.6 ± 12.9 W m^{-2} per unit optical depth. The scatter in the data on this forcing efficiency plot is partly due to varying aerosol composition throughout the measurement period. Moreover, the normal-incidence TOA irradiance decreases from about 1360 W m^{-2} at the beginning of the measurement period to about 1330 W m^{-2} at the end. Hence the total amount of energy incident the atmosphere in the region is varying.

[21] To account for the variability of the external flux, we examine the fractional forcing efficiency, ΔFF_e. Figure 5 depicts the fractional forcing as a function of τ_{500} completely analogous to Figure 4. The resulting values of ΔFF_e for the TSBR, FSBR, and visible band passes are -15.7 ± 3.3, -13.8 ± 3.5, and -21.8 ± 3.8. The units of these numbers are all percent of the TOA flux in that band pass per unit optical depth at 500 nm. We see here that despite the fact that ΔF_e for the FSBR and visible band passes are approximately equal in magnitude, the corresponding values of ΔFF_e indicate that a larger percentage for the visible portion of the solar spectrum is absorbed at Gosan during ACE-Asia.

[22] Similar analyses of ΔDF and ΔFDF in terms of τ_{AVE} give values for the diurnal forcing efficiency, ΔDF_e (see Figure 6), and the fractional diurnal forcing efficiency, ΔFDF_e (see Figure 7). A summary of all of the forcing efficiency results during at Gosan during ACE-Asia is given in Table 4.

4. Discussion

[23] To understand the aerosol forcing efficiency trends, it is beneficial to have a range of high and low aerosol conditions. The distribution of clear-sky aerosol optical depths at Gosan during ACE-Asia (Figure 2) shows that even though the majority of the measurements were made with τ_{500} in the range 0.3–0.5, there were also periods of

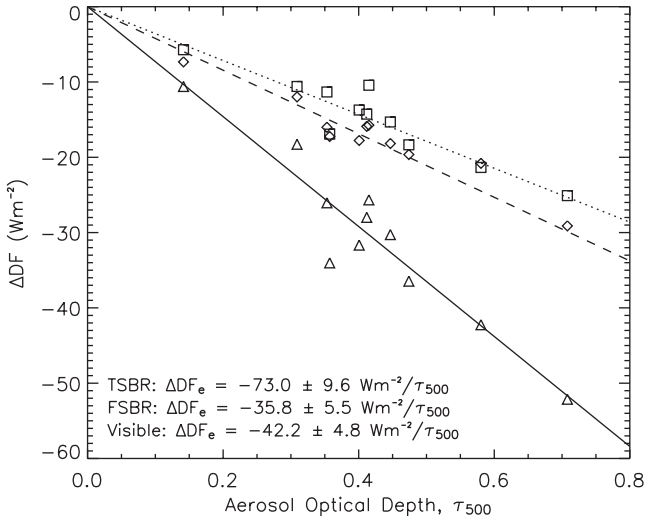

Figure 6. The diurnal forcing is plotted versus the average aerosol optical depth for the 11 clear or mostly clear days summarized in Table 3. The TSBR, FSBR, and visible band passes are triangles, squares, and diamonds, respectively. Additionally, the best fit lines are solid, dotted, and dashed, respectively.

relatively clean conditions ($\tau_{500} = 0.1 - 0.2$) as well as high aerosol events ($\tau_{500} = 0.6 - 0.8$). Low aerosol conditions are most useful in validating the components used in calculating the radiative forcing: the radiation measurements and the "no-aerosol" model calculations. These quantities must compare well for the calculated forcing to approach zero as the aerosol optical depth also approaches zero, the boundary condition in the forcing definition. Furthermore, a close comparison of the measured and modeled fluxes also acts as a validation of the absolute calibration constants of the radiometers. As depicted in Figure 3b, the flux measurements on 16 April (the lowest aerosol optical depth day at Gosan during ACE-Asia) very nearly approach the "no-aerosol" model calculations thus

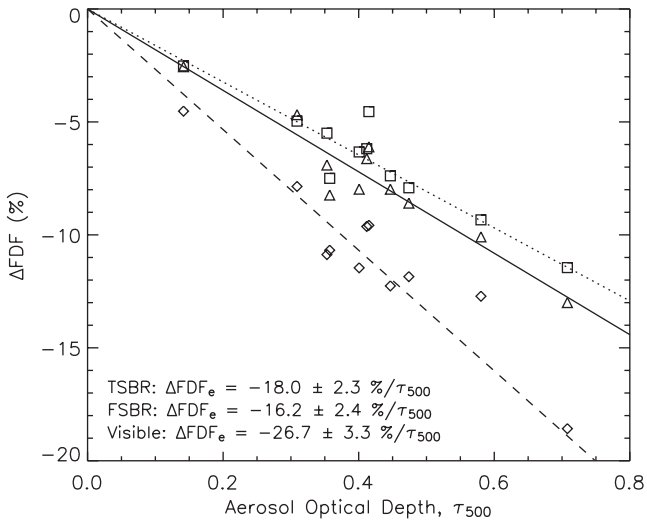

Figure 7. Same as Figure 6 but for the fractional diurnal forcing.

Table 4. Summary of Surface Forcing Efficiency Analyses at Gosan During ACE-Asia

Forcing Term	TSBR	FSBR	Visible
ΔF_e (W m^{-2})	−173.0 ± 32.9	−83.4 ± 21.0	−93.6 ± 12.9
ΔDF_e (W m^{-2})	−73.0 ± 9.6	−35.8 ± 5.5	−42.2 ± 4.8
ΔFF_e (%)	−15.7 ± 3.3	−13.8 ± 3.5	−21.8 ± 3.8
ΔFDF_e (%)	−18.0 ± 2.3	−16.2 ± 2.4	−26.7 ± 3.3

giving credibility to the model calculations and flux measurements.

[24] The surface forcing results discussed in this work represent the average of the overall conditions in Gosan from 25 March to 4 May 2001. Back trajectories of the air masses in the atmospheric column over Gosan indicate that the region was influenced by a number of different source regions throughout the measurement period and consequently a wide variety of aerosol types [*Merrill*, 2001]. The spread of the data points about the best fit lines in Figures 4 through 7 most likely represents the varying forcing efficiencies associated with these different aerosol types. Nevertheless, the overall effect of the aerosols in this region is properly characterized by the forcing efficiencies summarized in Table 4. As a consistency check, when all of the parameters presented in Table 4 are re-analyzed using the aerosol optical depth measurements from the CMDL, METRI, and AERONET platforms, the resulting values are all well within the quoted uncertainties.

[25] It is instructive not only to look at the magnitude of the radiative forcing due to atmospheric aerosols, but also the distribution within the solar spectrum of this energy. At Gosan, for the time period during ACE-Asia, even though the absolute radiative forcing at the surface in the visible and near-infrared portions of the solar spectrum are roughly equal (−93.6 and −83.4 W m$^{-2}/\tau_{500}$), the fraction relative to that incident the Earth's atmosphere is greater for the visible light (−21.8 and −13.8%/τ_{500}). Hence as expected, the aerosols have a much greater effect in perturbing the visible portion of the solar spectrum than the near-infrared portion.

[26] The Indian Ocean Experiment (INDOEX), in part, characterized the radiative forcing resulting from the anthropogenic haze in the North Indian Ocean and Southeast Asia [*Ramanathan et al.*, 2001]. The intensive field phase of INDOEX took place from February through March 1999. Independent measurements of ΔDF_e at the Kaashidhoo Climate Observatory (KCO) resulted in values of −70 to −75 W m$^{-2}/\tau_{AVE}$ for the total solar spectrum and about −38 to −40 W m$^{-2}/\tau_{AVE}$ for the visible (0.4–0.7 μm) [*Satheesh and Ramanathan*, 2000; *Bush and Valero*, 2002]. The magnitude of these forcing efficiencies is slightly less (about 5%) but still comparable (within error margins) to those found in this study for the ACE Asia domain (−73.0 and −42.2 W m$^{-2}/\tau_{AVE}$ for the same spectral regions).

[27] An additional analysis of the INDOEX surface forcing measurements presented by *Bush and Valero* [2002] specifically looking at the fractional forcing efficiencies gives values of −16.8 ± 1.2%/τ_{AVE} and −23.1 ± 2.6%/τ_{AVE} for ΔFDF_e in the TSBR and visible spectral regions. A comparison of the ACE-Asia and INDOEX surface forcing measurements is summarized in Table 5. When the geographic location and time of year that the surface measurements in ACE-Asia and INDOEX are

Table 5. Summary of Surface Forcing Efficiency Analyses at Gosan During ACE-Asia and at KCO During INDOEX

	ACE-Asia		INDOEX	
Forcing Term	TSBR	Visible	TSBR	Visible
ΔF_e (W m^{-2})	−173.0 ± 32.9	−93.6 ± 12.9	−173.8 ± 30.2	−88.7 ± 14.7
ΔDF_e (W m^{-2})	−73.0 ± 9.6	−42.2 ± 4.8	−72.2 ± 5.5	−38.5 ± 4.0
ΔFF_e (%)	−15.7 ± 3.3	−21.8 ± 3.8	−15.2 ± 2.6	−19.5 ± 4.3
ΔFDF_e (%)	−18.0 ± 2.3	−26.7 ± 3.3	−16.8 ± 1.2	−23.1 ± 2.6

considered, the average TOA flux is slightly greater for the INDOEX period (February through March 1999) relative to that for ACE-Asia (March through May 2001). This reduction in the TOA flux in ACE-Asia relative to the INDOEX case explains the larger values of ΔFF_e and ΔFDF_e for comparable values of ΔF_e and ΔDF_e.

[28] **Acknowledgments.** We greatly acknowledge the Korean Meteorological Administration and the Meteorological Research Institute for organization at the Jeju site, the University Corporation for Atmospheric Research (UCAR) for coordination and logistics associated with ACE-Asia, and personnel from the Atmospheric Research Laboratory, especially Sabrina Leitner and Shelly K. Pope, for assistance in calibrations, making the measurements, and all other aspects of making a field campaign successful. This research was supported by NSF grant ATM-0002210.

References

Anderson, G. P., et al., MODTRAN 4: Radiative transfer modeling for remote sensing, in *Optics in Atmospheric Propagation and Adaptive Systems III*, edited by A. Kohnle and J. D. Gonglewski, *Proc. SPIE Int. Soc. Opt. Eng., 3866*, 2–10, 1999.

Bates, T. S., Preface to special section: First Aerosol Characterization Experiment (ACE 1) Part 2, *J. Geophys. Res.*, *104*, 21,645–21,647, 1999.

Bates, T. S., B. J. Huebert, J. L. Gras, F. B. Griffiths, and P. A. Durkee, International Global Atmospheric Chemistry (IGAC) Projects First Aerosol Characterization Experiment (ACE 1): Overview, *J. Geophys. Res.*, *103*, 16,297–16,318, 1998.

Bush, B. C., and F. P. J. Valero, Spectral aerosol radiative forcing at the surface during the Indian Ocean Experiment (INDOEX), *J. Geophys. Res.*, *107*(D19), 8003, doi:10.1029/2000JD000020, 2002.

Bush, B. C., S. K. Pope, A. Bucholtz, F. P. J. Valero, and A. Strawa, Surface radiation measurements during the ARESE campaign, *J. Quant. Spectrosc. Radiat. Transfer*, *61*(2), 237–247, 1999.

Graham, N. E., Simulation of recent global temperature trends, *Science*, *267*, 666–671, 1995.

Hansen, J. E., M. Sato, A. Lacis, R. Ruedy, I. Tegen, and E. Matthews, Climate forcings in the industrial era, *Proc. Natl. Acad. Sci. U. S. A.*, *95*, 12,753–12,758, 1998.

Holben, B. N., et al., AERONET—A federated instrument network and data archive for aerosol characterization, *Remote Sens. Environ.*, *66*, 1–16, 1998.

Huebert, B. J., An overview of the ACE-Asia Aerosol Characterization Experiment intensive observations during the spring of 2001, *Eos Trans. AGU*, *82*(47), Fall Meet. Suppl., Abstract A32D-01, 2001.

Jayaraman, A., D. Lubin, S. Ramachandran, V. Ramanathan, E. Woodbridge, W. D. Collins, and K. S. Zalpuri, Direct observations of aerosol radiative forcing over the tropical Indian Ocean during the January–February 1996 pre-INDOEX cruise, *J. Geophys. Res.*, *103*, 13,827–13,836, 1998.

Merrill, J., ACE-Asia circulation and transport events and patterns, *Eos Trans. AGU*, *82*(27), Fall Meet. Suppl., Abstract A22A-0122, 2001.

Meywerk, J., and V. Ramanathan, Observations of the spectral clear-sky aerosol forcing over the tropical Indian Ocean, *J. Geophys. Res.*, *104*, 24,359–24,370, 1999.

Raes, F., T. Bates, F. McGovern, and M. Van Liedekerke, The 2nd Aerosol Characterization Experiment (ACE-2): General overview and main results, *Tellus Ser. B*, *52*(2), 111–125, 2000.

Ramanathan, V., et al., Indian Ocean Experiment, an integrated analysis of the climate forcing and effects of the great Indo-Asian haze, *J. Geophys. Res.*, *106*, 28,371–28,398, 2001.

Rodhe, H., The second Aerosol Characterization Experiment (ACE-2)—Foreword, *Tellus Ser. B*, *52*(2), 2000.

Satheesh, S. K., and V. Ramanathan, Large differences in tropical aerosol forcing at the top of the atmosphere and Earth's surface, *Nature*, *405*, 60–63, 2000.

Valero, F. P. J., and B. C. Bush, Measured and calculated clear-sky solar radiative fluxes during the Subsonic Aircraft Contrail and Cloud Effects Special Study (SUCCESS), *J. Geophys. Res.*, *104*, 27,387–27,398, 1999.

Valero, F. P. J., W. J. Y. Gore, and L. P. M. Giver, Radiative flux measurements in the troposphere, *Appl. Opt.*, *27*, 831–838, 1982.

Valero, F. P. J., A. Bucholtz, B. C. Bush, S. K. Pope, W. D. Collins, P. Flatau, A. Strawa, and W. J. Y. Gore, Atmospheric Radiation Measurements Enhanced Shortwave Experiment (ARESE): Experimental and data details, *J. Geophys. Res.*, *102*, 29,929–29,937, 1997.

Valero, F. P. J., S. K. Pope, B. C. Bush, Q. Nguyen, D. Marsden, R. D. Cess, A. S. Simpson-Leitner, A. Bucholtz, and P. M. Udelhofen, Absorption of solar radiation by the clear and cloudy atmosphere during the Atmospheric Radiation Measurement Enhanced Shortwave Experiments (ARESE) I and II: Observations and models, *J. Geophys. Res.*, *108*(D1), 4016, doi:10.1029/2001JD001384, 2003.

B. C. Bush and F. P. J. Valero, Atmospheric Research Laboratory, Scripps Institution of Oceanography, University of California, San Diego, La Jolla, CA 92093-0242, USA. (bcbush@ucsd.edu)